

Heterogeneous Photoreaction of Tetrachloroethene—Air Mixture on Halloysite Particles

SHUZO KUTSUNA,*
TAKASHI IBUSUKI, AND KOJI TAKEUCHI
National Institute for Resources and Environment, 16-3
Onogawa, Tsukuba, 305-8569, Japan

The heterogeneous photodegradation of tetrachloroethene in air proceeded on clay particles (halloysite) under photoillumination (>300 nm) with an induction period. The induction period and the tetrachloroethene removal rate were not sensitive to the tetrachloroethene partial pressure or the relative humidity. The photodegradation of tetrachloroethene was accelerated by the reaction with the released Cl atoms. Several tentative photoreaction mechanisms such as that via the tetrachloroethene—oxygen molecule charge-transfer complex were proposed based on the diffuse reflectance UV–vis spectra and the physical properties of the halloysite particles. The photoreaction rate was estimated on the basis of a simulated calculation, which can reproduce the tetrachloroethene initial pressure dependence versus time for tetrachloroethene and its degradation products.

Introduction

Tetrachloroethene ($\text{CCl}_2=\text{CCl}_2$) has been widely used as a solvent for metal parts, semiconductor washing, and dry cleaning. It causes groundwater pollution which poses a serious environmental problem (1). Since most of the $\text{CCl}_2=\text{CCl}_2$ used is emitted into the atmosphere, much attention has been given to its concentrations in the atmosphere from the standpoint of human health and welfare. The attack by the OH radicals is accepted as the dominant path for the tropospheric degradation of these volatile compounds. The lifetime of $\text{CCl}_2=\text{CCl}_2$ has been estimated at 140 days based on the reaction rate with OH (2).

Potential photoreactions on the atmosphere–soils interface may effect the movement of $\text{CCl}_2=\text{CCl}_2$ in the environment, though it is restricted to the upper millimeter of soils (3). In laboratory experiments, it has been pointed out that volatile compounds including $\text{CCl}_2=\text{CCl}_2$ adsorbed on particulate matter such as sand and silica are mineralized under photoillumination, even at wavelengths longer than 290 nm (4), but the intermediates in the heterogeneous photochemical reactions were not discussed. We investigated the heterogeneous photoreactions of $\text{CCl}_2=\text{CCl}_2$ and trichloroethene ($\text{CHCl}=\text{CCl}_2$) with TiO_2 particles and found these volatile compounds were decomposed fast enough to serve as a possible sink (5).

In this study, the heterogeneous reactions of $\text{CCl}_2=\text{CCl}_2$ were examined on two kinds of clay particles (kaolinite and halloysite) which are among the main components of soils (6, 7). $\text{CCl}_2=\text{CCl}_2$ was only decomposed by a heterogeneous photoreaction on the halloysite particles. The influence of

the reaction conditions such as temperature on the $\text{CCl}_2=\text{CCl}_2$ decay and the degradation product formation was examined. A possible reaction scheme was discussed on the basis of the characteristics of halloysite and diffuse reflectance UV–vis absorption spectra of halloysite particles exposed to a $\text{CCl}_2=\text{CCl}_2$ –air mixture. The contribution of Cl atoms released by the reaction to the photodegradation of $\text{CCl}_2=\text{CCl}_2$ on halloysite particles was also discussed.

Experimental Section

The experiments were performed in a closed-circulation reactor made of Pyrex glass. It contains a magnetically driven glass pump circulating the gas mixture and a multireflection long path cell with a 3 m path length interfaced to an FTIR spectrometer (JEOL, WINSPEC50). It was described elsewhere in more detail (8) except for the new removal cell (9). The total volume of the reactor was 0.85 dm^3 . The new removal cell was made from Pyrex glass with a quartz window. It has a loop injector with 12 ports. Clay particles were piled up loose in a small plate. The plate was set in the center of the loop injector on which a quartz plate was put to more efficiently expose the clay particles to the gas mixture. After the removal cell was connected to the closed-circulation reactor, its temperature was kept constant using a heater or temperature-controlled water bath.

A commercial grade reagent of $\text{CCl}_2=\text{CCl}_2$ (Wako Chemical, 99%) was used without further purification. The gas mixture of $\text{CCl}_2=\text{CCl}_2$ in air was prepared by evaporation of a liquid sample of $\text{CCl}_2=\text{CCl}_2$, followed by dilution with synthetic air (Takachiho Kagaku Co., 99.9999%) by measuring each partial pressure with an absolute pressure gauge (MKS Baratron 122AA). So was the gas mixture of trichloroethene ($\text{CHCl}=\text{CCl}_2$) by evaporation of a liquid sample (Wako Chemical, 99.5%). The gas mixture of 1,1-dichloroethene ($\text{CH}_2=\text{CCl}_2$) was prepared by mixing a standard gas mixture in nitrogen (Takachiho-Kogyo Co.) with oxygen. The humidified gas mixture was prepared by passing part of the gas mixture through water in a bottle (Ichinose-type humidifier).

The examined clay particles of kaolinite and halloysite were obtained from the Iwamoto Mineral Co. Their structure, BET surface area, and components are shown in Table 1. Table 1 does not include ignition loss, which mainly consisted of crystalline OH groups. The pretreatment of clay particles was carried out under a dry or humidified air flow. Fifty milligrams of clay particles placed in the removal cell was kept at a fixed temperature (typically 393 K) for an hour under $0.2 \text{ dm}^3 \text{ min}^{-1}$ of flowing synthetic air at atmospheric pressure and then cooled to the reaction temperature (typically 298 K). In the experiment carried out under a humidified atmosphere, the clay particles were followed by exposure to $0.2 \text{ dm}^3 \text{ min}^{-1}$ of the synthetic air humidified at a definite relative humidity for an additional 1 h at the reaction temperature.

The experimental procedure was divided into the following three steps. During the initial 30 min, the reactant gas mixture was circulated without contact to the clay particles. Subsequently, the gas-circulating route was changed so that the gas mixture flowed over the clay particles in the dark for 1 h. Finally, photoillumination with light of a wavelength longer than 300 or 360 nm was carried out using a 500 W xenon short arc lamp (Ushio Co.) and a UV30 or L38 optical filter (Hoya Co.), respectively. The measured intensity was about 6 mW cm^{-2} at 365 nm using a UV sensor (USHIO, UVD-365PD). The reaction temperature was set between 283 and 313 K by putting the removal cell in a temperature-controlled water bath.

* Corresponding author phone: 81-298-61-8163; fax: 81-298-61-8158; e-mail: kutsuna@nire.go.jp.

TABLE 1. Properties of the Examined Clays

	structure	BET area/m ² g ⁻¹	chemical component/wt %								
			SiO ₂	Al ₂ O ₃	Fe ₂ O ₃	TiO ₂	K ₂ O	CaO	Na ₂ O	MgO	water ^a
kaolinite	thin leaf	16.0	40.5	36.1	0.1	0.5	2.1	0.1			0.5
halloysite	tube	29.4	50.4	35.7	0.2	0.1	trace	0.0	0.2	0.0	2.6

^a Water contents were calculated from the decrement of the weight by heating clay particles at 473 K for 2 h in ambient air.

The IR spectra of CCl₂=CCl₂ and its degradation products were measured at a 0.5 cm⁻¹ resolution with 50 accumulations. The absolute concentration measurements of CCl₂=CCl₂, CO₂, and CO were based on the calibration curves which were prepared based on the IR peak areas (PA) of the concentration-prepared standard gases. The peak areas for the region of 890.0–939.9 cm⁻¹ (PA1), 2290.1–2389.9 cm⁻¹ (PA2), and 2050.0–2230.1 cm⁻¹ (PA3) were used for the quantification of CCl₂=CCl₂, CO₂, and CO, respectively. The absorption coefficients (base 10) were 3.60 × 10⁻⁴ mTorr⁻¹ cm⁻² for PA1 of CCl₂=CCl₂ and 1.31 × 10⁻⁴ mTorr⁻¹ cm⁻² for PA3 of CO. The partial pressure of CO₂ (P_{CO2}/mTorr) was calculated based on the calibration curve that P_{CO2} = 2.15 × PA2 + 0.0661 × PA2² + 0.00034 × PA2³ for the 3 m path length. The absolute concentration measurements of COCl₂ and HCl were based on the published absorption coefficient (base 10) of 2.00 × 10⁻⁵ mTorr⁻¹ cm⁻¹ for the 1832.3 cm⁻¹ peak of COCl₂ and 2.40 × 10⁻⁶ mTorr⁻¹ cm⁻¹ for the maximum peak in the region of 2740.1 to 2715.1 cm⁻¹ of HCl (10). For CCl₃C(O)Cl, we used the measurement of the pressure-prepared gas mixture. Since the IR peaks of HCl were also measured, the prepared partial pressure was corrected by subtracting the partial pressure of HCl in order to deduce the partial pressure of CCl₃C(O)Cl. The absorption coefficient of 7.03 × 10⁻⁶ mTorr⁻¹ cm⁻¹ for the 1026.9 cm⁻¹ peak of CCl₃C(O)Cl was obtained. Since COCl₂ also shows an IR absorption at 1026.9 cm⁻¹, the absorbance of CCl₃C(O)Cl was corrected by subtracting that of COCl₂, that is, the value of 0.013 × (OD at 1832.3 cm⁻¹).

The CCl₂=CCl₂ or its degradation products adsorbed on clay particles were measured with a diffuse reflectance UV–vis spectrometer. The diffuse reflectance UV–vis absorption spectra were measured using a flat quartz cell and a spectrometer (Hitachi Co., U-3500) equipped with an internal diffuse reflectance attachment. A pellet of MgSO₄ was used as the reference. The pretreatment of clay particles and/or the introduction of the gas mixture in a flat quartz cell were carried out using a glass vacuum line. The clay particles were evacuated at liquid nitrogen temperature in order to prevent the water content being releasing from them, and then at room temperature they were exposed to 620 Torr of synthetic air. Under 620 Torr of air atmosphere they were heated at 393 K for an hour and cooled to ambient temperature. They were again evacuated at liquid nitrogen temperature and then placed in the spectrometer and measured at ambient temperature. After a sample of clay particles in a vacuum was measured, it was exposed to the CCl₂=CCl₂–air mixture at a specific pressure using a glass vacuum line for the subsequent measurement.

Results and Discussion

Photodegradation of CCl₂=CCl₂ on Halloysite Particles.

Figure 1 shows the change in the CCl₂=CCl₂ partial pressure in the experiment when the CCl₂=CCl₂–air mixture flowed over no clay particles and the halloysite or kaolinite particles. The decrease in partial pressure at 30 min was the sum of the decrease due to the adsorption onto the clay particles and the decrease due to the dilution attending the change of the gas-circulating route. The latter corresponds to a 23% decrease in partial pressure. The amount of adsorption on

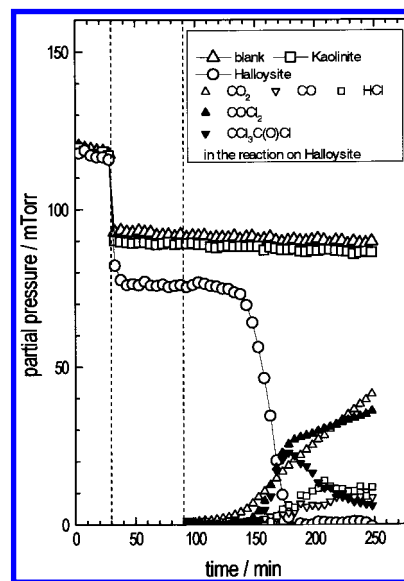


FIGURE 1. Time-course of CCl₂=CCl₂ partial pressure in air without clays, with kaolinite or halloysite particles at 298 K. The partial pressure of the degradation products in the experiment with halloysite particles is also plotted. The gas-circulating route was changed at 30 min to expose clay particles to the gas mixture. Illumination (>300 nm) was started at 90 min.

the halloysite particles was much greater than that on the kaolinite particles. In the dark, the CCl₂=CCl₂ partial pressure did not change. Under photoillumination, CCl₂=CCl₂ partial pressure remained almost constant in both cases without clay particles and with the kaolinite particles. However, for the halloysite particles, the CCl₂=CCl₂ partial pressure slightly decreased during the initial 1 h of photoillumination and then rapidly decreased.

Figure 2 shows the IR spectra of the CCl₂=CCl₂ gas mixture on halloysite particles before photoillumination and at 78 min and 158 min of photoillumination. Trichloroacetyl chloride (CCl₃C(O)Cl), phosgene (COCl₂), carbon dioxide (CO₂), carbon monoxide (CO), and hydrogen chloride (HCl) were detected as the degradation products. Figure 1 also shows the change in the partial pressure of these degradation products for halloysite particles. CCl₃C(O)Cl and COCl₂ increased as the CCl₂=CCl₂ rapidly decreased after the induction period. CCl₃C(O)Cl decreased after almost all of CCl₂=CCl₂ was consumed.

Diffuse Reflectance UV–vis Spectra of Clay Particles Exposed to CCl₂=CCl₂–Air Mixture. Figure 3 shows the diffuse reflectance UV–vis spectra of halloysite and kaolinite particles in a vacuum and under the CCl₂=CCl₂–air mixture. Both the halloysite and kaolinite particles have absorptions in the wavelength range longer than 300 nm. Although the CCl₂=CCl₂ absorption spectrum in the gas phase is shorter than 240 nm (11), a broad absorption between 250 and 400 nm was observed only for the case of the halloysite particles (spectrum c in Figure 3). An explanation of this absorption is that it was due to the absorption of the CCl₂=CCl₂–O₂ charge-transfer complex in the electrostatic field of the halloysite layer analogous to the alkene–O₂ charge-transfer

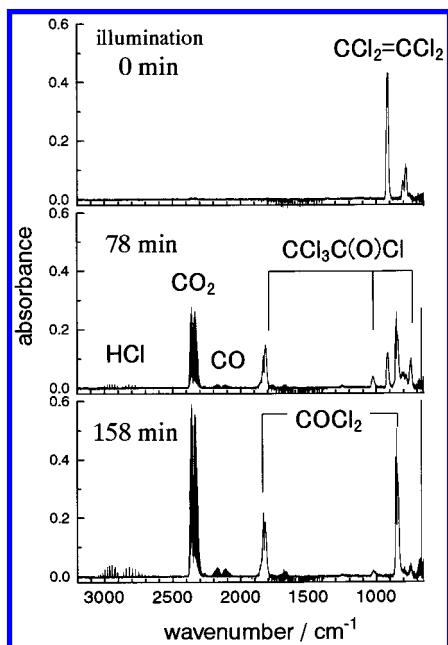


FIGURE 2. IR spectra of $\text{CCl}_2=\text{CCl}_2$ -air mixture on halloysite particles before photoillumination and at 78 min and 158 min photoillumination (>300 nm) at 298 K.

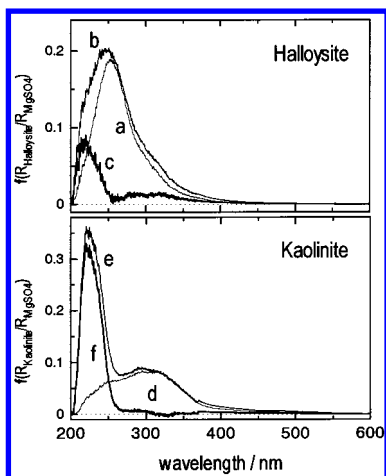


FIGURE 3. Diffuse reflectance UV-vis absorption spectra of halloysite (upper) and kaolinite (lower) particles. Spectra *a*, *d* and *b*, *e* were measured in a vacuum and in the presence of $\text{CCl}_2=\text{CCl}_2$ (9.3 Torr) in air (620 Torr), respectively. Spectra *c* and *f* are the subtracted spectra of (*b* - *a*) and (*e* - *d*), respectively. The ordinate indicates the Kubelka-Munk function.

complex in zeolite (12). The electric static field could be stronger in halloysite particles than in kaolinite particles due to the amphoteric nature of the layer in halloysite (13).

Dependence of $\text{CCl}_2=\text{CCl}_2$ Decay and the Degradation Product Formation on the Reaction Conditions. Figure 4 shows the time-course of the $\text{CCl}_2=\text{CCl}_2$ partial pressure in humidified air (B) and when the pretreatment temperature of the halloysite particles was 333 K (C). Both time-profiles were similar to that with halloysite particles pretreated at 393 K and in dry air (A), indicating that the photodegradation rate was not sensitive to either the pretreatment temperature or the relative humidity appropriate to the atmosphere.

Figure 5 shows the time-course of the $\text{CCl}_2=\text{CCl}_2$ residence ratio, CO_2 partial pressure, the formation ratio of $\text{CCl}_3\text{C}(\text{O})\text{Cl}$ and COCl_2 to the $\text{CCl}_2=\text{CCl}_2$ decay at different partial pressures of $\text{CCl}_2=\text{CCl}_2$. The $\text{CCl}_2=\text{CCl}_2$ residence ratio decay was not sensitive to the $\text{CCl}_2=\text{CCl}_2$ partial pressure. Its rate was rather high at the lower $\text{CCl}_2=\text{CCl}_2$ partial pressure except

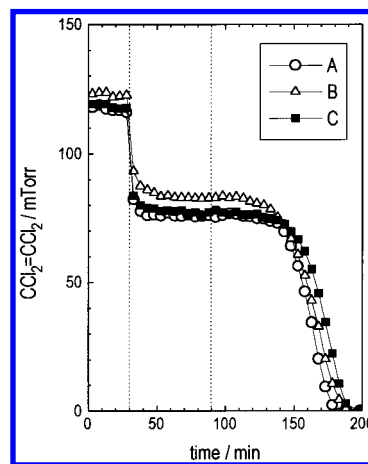


FIGURE 4. Dependence on the relative humidity or the pretreatment temperature for $\text{CCl}_2=\text{CCl}_2$ -air-halloysite at 298 K. Plots A and C were examined under dry conditions, and plot B was examined at 40%RH. Plots A and B were examined on halloysite particles pretreated at 393 K, and plot C was examined on those pretreated at 333 K. Illumination (>300 nm) was started at 90 min.

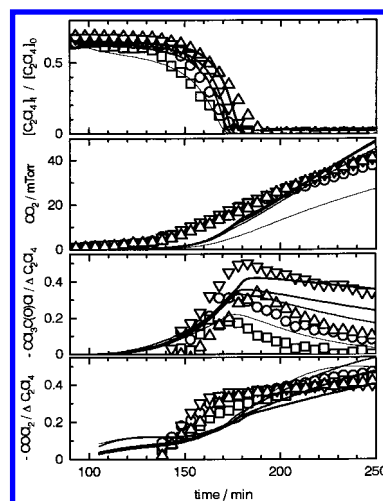


FIGURE 5. The dependence on the partial pressure of $\text{CCl}_2=\text{CCl}_2$ in the reaction of $\text{CCl}_2=\text{CCl}_2$ -air mixture on halloysite particles at 298 K. Illumination (>300 nm) was started at 90 min. The symbols of \square , \circ , \triangle and ∇ indicate the result of the $\text{CCl}_2=\text{CCl}_2$ partial pressure at 0 min ($[\text{C}_2\text{Cl}_4]_0$) of 46, 117, 166 and 268 mTorr, respectively. The lines of \square , \circ , \triangle , and ∇ indicate the calculated results based on the scheme shown in Table 2 for $[\text{C}_2\text{Cl}_4]_0$ of 46, 117, 166, and 268 mTorr, respectively.

for the relation between 166 and 268 mTorr of $\text{CCl}_2=\text{CCl}_2$. CO_2 formation rate was independent of the $\text{CCl}_2=\text{CCl}_2$ partial pressure. The formation ratio of $\text{CCl}_3\text{C}(\text{O})\text{Cl}$ increased with the increasing $\text{CCl}_2=\text{CCl}_2$ partial pressure, while that of COCl_2 was almost constant.

The temperature dependence was examined in the range of 283–313 K. The photodegradation rate was not sensitive to the reaction temperature. The CO_2 formation rate is dependent upon the reaction temperature and increased with increasing temperature. The formation ratio of $\text{CCl}_3\text{C}(\text{O})\text{Cl}$ and COCl_2 was not sensitive to the reaction temperature.

Contribution of Cl Atoms Released to the Photodegradation of $\text{CCl}_2=\text{CCl}_2$. The time-profile of the $\text{CCl}_2=\text{CCl}_2$ decay, that is, the rapid decrease after the induction time, suggests that the photoreaction may include an autocatalytic process in which the released Cl atoms attack $\text{CCl}_2=\text{CCl}_2$. To confirm this, the photoreaction was examined in the presence of ethene ($\text{CH}_2=\text{CH}_2$) as a scavenger of Cl atoms. Although $\text{CH}_2=\text{CH}_2$ did not decay by itself on the halloysite particles

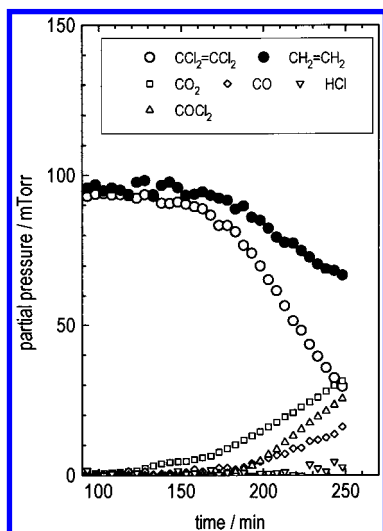


FIGURE 6. Time-course of the partial pressure of $\text{CCl}_2=\text{CCl}_2$, $\text{CH}_2=\text{CH}_2$, and their degradation products for $\text{CCl}_2=\text{CCl}_2-\text{CH}_2=\text{CH}_2$ -air-halloysite at 298 K. Illumination (> 300 nm) was started at 90 min.

in air during photoillumination (> 300 nm), it decreased in the presence of $\text{CCl}_2=\text{CCl}_2$ as shown in Figure 6. The decay rate of $\text{CCl}_2=\text{CCl}_2$ was smaller, and the induction time was longer than in the case shown in Figure 1. The formation of $\text{CCl}_3\text{C}(\text{O})\text{Cl}$ was not observed in the gas phase. This result indicates that part of the Cl atoms released from $\text{CCl}_2=\text{CCl}_2$ attacked $\text{CH}_2=\text{CH}_2$ so that the reaction of the Cl atoms with $\text{CCl}_2=\text{CCl}_2$ was restricted. The expected products such as $\text{CH}_2\text{ClC}(\text{O})\text{H}$ due to the reaction of Cl atoms with $\text{CH}_2=\text{CH}_2$ were probably not observed because of their further decomposition.

The point concerning atmospheric chemistry is whether Cl atoms will go into the gas phase or not. If all the Cl atoms were released from the clay particles, they will be diluted in the environment to a concentration at which the reaction with them may be insignificant. This can be estimated from the relative ratio of the $\text{CCl}_2=\text{CCl}_2$ decay rate to the $\text{CH}_2=\text{CH}_2$ decay rate (R). Since the decay rate of $\text{CCl}_2=\text{CCl}_2$ or $\text{CH}_2=\text{CH}_2$ is 0.82 ± 0.01 mTorr min^{-1} or 0.37 ± 0.01 mTorr min^{-1} , respectively, from the slope of each line which was linearly fitted with regard to the data after 180 min, the observed ratio of the $\text{CCl}_2=\text{CCl}_2$ decay rate to the $\text{CH}_2=\text{CH}_2$ decay rate (R_{obs}) is 2.2. On the other hand, the ratio (R_{gas}) is estimated to be less than 1.1 when the reaction of Cl atoms with $\text{CCl}_2=\text{CCl}_2$ or $\text{CH}_2=\text{CH}_2$ occurred only in the gas phase.

$$R_{\text{gas}} = \frac{(k_{\text{CCl}_2=\text{CCl}_2}^{\text{Cl}}[\text{Cl}][\text{CCl}_2=\text{CCl}_2])}{(k_{\text{CH}_2=\text{CH}_2}^{\text{Cl}}[\text{Cl}][\text{CH}_2=\text{CH}_2])} < 1.1$$

The gas-phase reaction rate constant with the Cl atom of $\text{CCl}_2=\text{CCl}_2$ ($k_{\text{CCl}_2=\text{CCl}_2}^{\text{Cl}}$) or $\text{CH}_2=\text{CH}_2$ ($k_{\text{CH}_2=\text{CH}_2}^{\text{Cl}}$) is $(2.6-4.5) \times 10^{-11}$ and $(0.4-1.7) \times 10^{-10}$ cm^3 molecule $^{-1}$ s $^{-1}$ at 298 K (14), respectively. The result of $R_{\text{obs}} > R_{\text{gas}}$ indicates that the reaction of $\text{CCl}_2=\text{CCl}_2$ proceeds not only in the gas-phase but also in the small pores and/or on the surface of the halloysite particles before they go into the gas phase. Since the amount of $\text{CCl}_2=\text{CCl}_2$ adsorption onto the halloysite particles was much greater than that of $\text{CH}_2=\text{CH}_2$, R_{obs} can be larger than R_{gas} . Hence, the contribution of Cl atoms to the photodegradation of $\text{CCl}_2=\text{CCl}_2$ can be worth evaluating although coexisting substances could interfere with it in the environment.

Reaction Scheme of Photodegradation of $\text{CCl}_2=\text{CCl}_2$ on Halloysite Particles. Though the rapid decrease after the induction time was mainly caused by the attack of Cl atoms as already mentioned, the initial step of the photoreaction

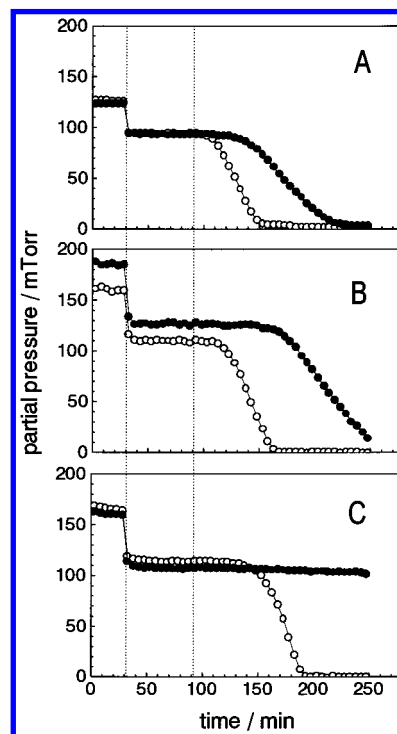


FIGURE 7. Time-course of the partial pressure of $\text{CH}_2=\text{CCl}_2$ (A), $\text{CHCl}=\text{CCl}_2$ (B), and $\text{CCl}_2=\text{CCl}_2$ (C) in air through the reaction on the halloysite particles at 298 K under photoillumination at wavelengths longer than 300 nm (open circle) or 360 nm (closed circle). Illumination was started at 90 min.

seems unclear. The diffuse reflectance UV-vis spectra shown in Figure 3 suggests that the absorption of light by the $\text{CCl}_2=\text{CCl}_2-\text{O}_2$ charge-transfer complex in the electrostatic field of the halloysite layer may initiate the reaction. On the other hand, since clay particles can absorb light with wavelengths shorter than 400 nm, a photosensitized reaction is also a possible mechanism. If the acid sites such as defects on the clay surfaces served active sites for the photoreaction, the presence of the water content would interfere with the reaction (9). However, the photoreaction rate was insensitive to the relative humidity as shown in Figure 4. An additional possible scheme was that photocatalytic components such as titanium dioxide might initiate the photodecomposition of $\text{CCl}_2=\text{CCl}_2$. The anatase type of titanium dioxide was reported as a component in kaolinite particles (15). For the latter two possible mechanisms, it is not clear why the reaction did not proceed on kaolinite particles. We also examined the heterogeneous photodegradation of $\text{CHCl}=\text{CCl}_2$ or $\text{CH}_2=\text{CCl}_2$. The heterogeneous photodegradation of $\text{CHCl}=\text{CCl}_2$ or $\text{CH}_2=\text{CCl}_2$ proceeded not only on the halloysite particles but also on the kaolinite particles where the decreasing rate was less and the induction period was longer than for the halloysite particles. These results suggested that the kaolinite particles also had a photochemical activity, which was lower than the halloysite particles. Figure 7 plots the partial pressures of three kinds of chloroethenes against the period of the photoillumination at wavelengths longer than 300 or 360 nm for the halloysite particles. Under photoillumination (> 360 nm), $\text{CCl}_2=\text{CCl}_2$ did not decrease for 3 h, and the decreasing rates of $\text{CHCl}=\text{CCl}_2$ and $\text{CH}_2=\text{CCl}_2$ were less, and their induction periods were longer than under photoillumination (> 300 nm). It seems that the rate-determining step may be correlated to the extent to which chloroethenes served as an electron donor, but it is still unclear as to which of the above three possible mechanisms initiated the reaction.

TABLE 2. Schemes of Photoreaction of CCl₂=CCl₂-Air-Halloysite Particles

reaction scheme	rate constant / min ⁻¹ or mTorr ⁻¹ min ⁻¹
CCl ₂ =CCl ₂ ⇌ CCl ₂ =CCl _{2ad} (1)	f: 1.1x10 ⁻¹¹ s n _s γ _{1a} Q ₁ ; r: 1.1x10 ²¹ / n _s ^{†1}
CCl ₂ =CCl _{2ad} → CCl ₂ =CCl _{2ad} (P) (2)	0.1 P ₁ ^{†2}
CCl ₂ =CCl _{2ad} (P) + O ₂ → CCl ₂ =CClO _{2ad} + ·Cl _{ad} (3)	k ₃ [O ₂] = 6x10 ⁻³
CCl ₂ =CClO _{2ad} → COCl _{2ad} + ·C(O)Cl _{ad} (4)	1
·C(O)Cl _{ad} → CO + Cl _{ad} (5)	2x10 ² ^{†3}
·C(O)Cl _{ad} + O ₂ → ·C(O)ClO _{2ad} (6)	5.3x10 ⁻³ ^{†3}
RO _{2ad} · + R'O _{2ad} · → RO _{ad} · + R'O _{ad} · + O ₂ (7; R,R':C(O)Cl) (11; R,R':CCl ₃ CCl ₂)	10 ⁻²
(15; R,R':CCl ₃) (32; R,R':CCl ₃ C(O)) (38; R:C(O)Cl, R':CCl ₃ CCl ₂) (39; R:C(O)Cl, R':CCl ₃) (40; R:C(O)Cl, R':CCl ₃ C(O)) (41; R:CCl ₃ CCl ₂ , R':CCl ₃) (42; R:CCl ₃ CCl ₂ , R':CCl ₃ C(O)) (43; R:CCl ₃ , R':CCl ₃ C(O))	
·C(O)ClO → CO ₂ + ·Cl _{ad} (8)	10 ²
CCl ₂ =CCl _{2ad} + ·Cl _{ad} → CCl ₃ CCl _{2ad} (9)	1
CCl ₃ CCl _{2ad} + O ₂ → CCl ₃ CCl ₂ O _{2ad} · (10)	1
CCl ₃ CCl ₂ O _{2ad} · → CCl ₃ C(O)Cl _{ad} + ·Cl _{ad} (12)	90 ^{†4}
CCl ₃ CCl ₂ O _{2ad} · → CCl _{3ad} + COCl _{2ad} (13)	10 ^{†4}
·CCl _{3ad} + O ₂ → CCl ₃ O _{2ad} (14)	1
CCl ₃ O _{2ad} · → COCl _{2ad} + ·Cl _{ad} (16)	10 ²
CCl ₃ C(O)Cl _{ad} ⇌ CCl ₃ C(O)Cl (17)	f: 1.3x10 ²⁰ / n _s ; r: 1.0x10 ⁻¹¹ s n _s γ _{17a} Q ₁ ^{†1}
COCl _{2ad} ⇌ COCl ₂ (18)	f: 9.4x10 ²⁰ / n _s ; r: 1.4x10 ⁻¹¹ s n _s γ _{18a} Q ₁ ^{†1}
·Cl _{ad} ⇌ ·Cl (19)	f: 1.9x10 ¹⁵ / n _s ; r: 2.3x10 ⁻¹¹ s n _s γ _{19a} Q ₁ ^{†1}
CCl ₂ =CCl ₂ + ·Cl → CCl ₃ CCl ₂ · (20)	1.3x10 ² ^{†5}
CCl ₃ CCl ₂ · + O ₂ → CCl ₃ CCl ₂ O ₂ · (21)	1
2CCl ₃ CCl ₂ O ₂ · → 2CCl ₃ CCl ₂ O· + O ₂ (22)	51 ^{†6}
CCl ₃ CCl ₂ O· → CCl ₃ C(O)Cl + Cl (23)	75 ^{†7}
CCl ₃ CCl ₂ O· → CCl ₃ · + COCl ₂ (24)	25 ^{†7}
CCl ₃ · + O ₂ → CCl ₃ O ₂ · (25)	1
2CCl ₃ O ₂ · → 2CCl ₃ O· + O ₂ (26)	51 ^{†6}
CCl ₃ O· → COCl ₂ + ·Cl (27)	10 ³
CCl ₃ C(O)Cl _{ad} + S → CCl ₃ C(O)Cl _{ad} (S) (28)	0.1 S ₁ ^{†8}
CCl ₃ C(O)Cl _{ad} (S) → CCl ₃ C(O)Cl _{ad} · + ·Cl _{ad} + S (29)	0.2
CCl ₃ C(O)Cl _{ad} · → CCl _{3ad} · + CO (30)	2x10 ² ^{†3}
CCl ₃ C(O)Cl _{ad} · + O ₂ → CCl ₃ C(O)O ₂ · (31)	5.3x10 ⁻³ ^{†3}
CCl ₃ C(O)O ₂ · → CCl _{3ad} · + CO ₂ (33)	10 ³
COCl _{2ad} · + S → COCl _{2ad} (S) (34)	0.1 S ₁ ^{†8}
COCl _{2ad} (S) → C(O)Cl _{ad} · + ·Cl _{ad} + S (35)	0.2
·Cl _{ad} + surface species → HCl _{ad} (36)	10 ⁻²
HCl _{ad} ⇌ HCl (37)	f: 9.3x10 ¹⁹ / n _s ; r: 2.3x10 ⁻¹¹ s n _s γ _{37a} Q ₁ ^{†1}

^{†1} s: surface area of clay particles per unit volume; n_s: adsorption site density; γ_{ia}: accommodation coefficient; Q₁: ratio of unoccupied sites to n_s. s = 17.3 cm² cm⁻³. n_s is assumed to be 10¹⁵ cm⁻². γ_{ia} is assumed to be 1. ^{†2} P₁ is the ratio of unoccupied sites to n_{ps}. n_{ps} is the adsorption site density where CCl₂=CCl₂ can be photochemically activated. n_{ps} is assumed to be 2 orders of magnitude smaller than n_s. ^{†3} The branching ratio of 5/6 or 30/31 was fitted to reproduce the formation ratio of CO₂/CO. ^{†4} The branching ratio of 12/13 was fitted to reproduce the formation ratio of CCl₃C(O)Cl/COCl₂. ^{†5} The rate constant was referred to the literature (14). ^{†6} The reaction rate of 26 was referred to the literature (18). That of 22 was assumed to be equal to that of 26. ^{†7} The branching ratio of 23/24 was referred to the literature (2). ^{†8} S₁ is the ratio of unoccupied sites to n_{ss}. n_{ss} is the adsorption site density where CCl₃C(O)Cl or COCl₂ can be oxidized. n_{ss} was assumed to be 2 orders of magnitude smaller than n_s.

In the experiment where the photoillumination was restarted after the CCl₂=CCl₂-air mixture flowed over halloysite particles for 40 min under photoillumination and for 1 h in the dark, the CCl₂=CCl₂ decreased just after photoillumination. This indicates that the degradation intermediates capable of emitting Cl atoms accumulated on the halloysite particles at 298 K.

A tentative reaction scheme suitable to the CCl₂=CCl₂ partial pressure dependence shown in Figure 5 is shown in Table 2. The reaction of CCl₂=CCl₂ with O₂ in the electrostatic field of the halloysite particles was assumed as the initial step of the photoreaction. The intermediate of CCl₂=CClO₂ was adopted from analogy with the gas-phase or liquid-phase reactions (16, 17). Most of the reactions referred to the gas-phase reactions, and the scheme may include inadequate ones and/or overlook some reactions. Nevertheless, the scheme could reproduce the observed time-profile of the gas-phase species and play a part in evaluating the contri-

bution to the CCl₂=CCl₂ decay of the photodecomposition or the reaction with Cl as described below.

On the basis of this scheme, the time-profile of CCl₂=CCl₂ and its degradation products was simulated using the commercial software program FACSIMILE (AEA Technology). In Table 2, the subscript "ad" indicates the species adsorbed on the surface. The (P) value indicates CCl₂=CCl₂ adsorbed on the sites where CCl₂=CCl₂ can be photochemically activated. That of (S) indicates CCl₃C(O)Cl or COCl₂ adsorbed on the sites where they can be oxidized. Until these concepts were introduced into the reaction scheme, the CCl₂=CCl₂ pressure dependence of the induction period in the CCl₂=CCl₂ decay and the formation rates of CO₂ and COCl₂ could not be reproduced. The calculated results are plotted by lines in Figure 5.

On the basis of the simulated calculation, each contribution to the CCl₂=CCl₂ decay of the photodecomposition (reaction 3 in the scheme), the surface reaction with Cl ((9)

and the gas-phase reaction with Cl ((20)), was calculated to be 11, 78, and 3%; 5, 88, and 4%; 3, 90, and 4%; 2, 92, and 5%, for the $\text{CCl}_2=\text{CCl}_2$ initial pressure of 46, 117, 166, and 268 mTorr, respectively. It proved that $\text{CCl}_2=\text{CCl}_2$ was mostly decomposed by the surface reaction with Cl atoms which were released through the decomposition of $\text{CCl}_2=\text{CCl}_2$ and/or its degradation products. For the environmental soils, part of the Cl atoms released could react with coexisting species and hence the reactions of $\text{CCl}_2=\text{CCl}_2$ with Cl could be restricted. The examination of the influence of coexisting materials to the reaction of $\text{CCl}_2=\text{CCl}_2$ with Cl still remains as a subject to evaluate the reaction rate in the environment.

If the reactions with Cl are completely restricted, the $\text{CCl}_2=\text{CCl}_2$ decay will be determined only by the photodecomposition. In that case, the removal rate constant of gaseous $\text{CCl}_2=\text{CCl}_2$ is represented as $k_{sf} [\text{O}_2] (k_{If}/k_{Ir})(n_{ps}/n_s) s$. Its maximum value, which corresponds to $Q_I = 1$, is calculated to be $6 \times 10^{-7} s \text{ min}^{-1}$ using the values shown in Table 2 where s is the surface area of clay particles per unit volume ($\text{cm}^2 \text{ cm}^{-3}$) in the environment. It corresponds to $(2400/s)$ days of lifetime by assuming that the sunlight duration is half a day. If the air mass under 1 m height on the ground is considered, w wt % (percent by weight) of halloysite particles in the soil at ground level corresponds to $7.5 w \text{ cm}^2 \text{ cm}^{-3}$ of s based on the assumption that the density of the soils is 2.5 g cm^{-3} ; sunlight reached the upper 1 mm of the soils. Accordingly, the lifetime of $\text{CCl}_2=\text{CCl}_2$ in the air mass can be estimated as $(320/w)$ days. Since the atmospheric lifetime of $\text{CCl}_2=\text{CCl}_2$ through the gas-phase reaction with OH radicals is 140 days, potential photoreactions on the atmosphere-soils interface may effect the movement of $\text{CCl}_2=\text{CCl}_2$ in the environment in the case that soils contain several to tens wt % of reactive clays such as the halloysite particles examined. The dependence on the sunlight intensity and the interference of coexisting species such as organic acids in the soils are remaining subjects in order to estimate the role of the photoreactions of $\text{CCl}_2=\text{CCl}_2$ on clay particles in the environment.

Literature Cited

- (1) Smith, J. A.; Cary, T. C.; Kammer, J. A.; Kile, D. E. *Environ. Sci. Technol.* **1990**, *24*, 676.

- (2) Tuazon, E. C.; Atkinson, R.; Aschmann, S. M.; Goodman, M. A.; Winer, A. M. *Int. J. Chem. Kinet.* **1988**, *20*, 241.
- (3) Miller, G. C.; Hebert, V. R.; Miller, W. W. In *Reactions and Movement of Organic Chemicals in Soils*; SSSA Special Publication No. 22; Sawhney, B. L., Brown, K., Eds.; Madison, WI, 1989; pp 99–110.
- (4) Gab, S.; Schmitzer, J.; Thamm, H. W.; Parlar, H.; Korte, F. *Nature* **1977**, *270*, 331.
- (5) Kutsuna, S.; Ebihara, Y.; Nakamura, K.; Ibusuki, T. *Atmos. Environ.* **1993**, *27A*, 599.
- (6) Saigusa, M. In *Soil Chemistry*; Japan Chemical Society, Ed.; Gakkai Shuppan Center: Tokyo, 1989; Chapter 5.
- (7) Zielke, R. C.; Pinnavaia, T. J.; Mortland, M. M. In *Reactions and Movement of Organic Chemicals in Soils*; SSSA Special Publication No. 22; Sawhney, B. L., Brown, K., Eds.; Madison, WI, 1989; pp 81–97.
- (8) Kutsuna, S.; Toma, M.; Takeuchi, K.; Ibusuki, T. *Environ. Sci. Technol.* **1999**, *33*, 1071.
- (9) Kutsuna, S.; Takeuchi, K.; Ibusuki, T., *J. Geophys. Res.* **2000**, *105*, 6611.
- (10) Hanst, P. L.; Hanst, S. T. *Quantitative Reference Spectra for Gas Analysis*; Infrared Analysis Inc.; CA, 1990.
- (11) Berry, M. J. *J. Chem. Phys.* **1974**, *61*, 3114.
- (12) Blatter, F.; Frei, H. *J. Am. Chem. Soc.* **1993**, *115*, 7501.
- (13) Theng, B. K. G. *The Chemistry of Clay-Organic Reactions*; Adam Hilger: London, 1974; Chapter 1.
- (14) DeMore, W. B.; Sander, S. P.; Golden, D. M.; Hampson, R. F.; Kurylo, M. J.; Howard, C. J.; Ravishankara, A. R.; Kolb, C. E.; Molina, M. J. *Chemical Kinetics and Photochemical Data for Use in Stratospheric Modeling*; Evaluation No. 12, JPL Publication 97-4; Pasadena, CA, 1997.
- (15) Murad, E. *Am. Mineralogist* **1997**, *82*, 203.
- (16) Calderwood, T. S.; Neuman, R. C., Jr.; Sawyer, D. T. *J. Am. Chem. Soc.* **1983**, *105*, 3337.
- (17) Russell, J. J.; Seetula, J. A.; Gutman, D.; Senkan, S. M. *J. Phys. Chem.* **1989**, *93*, 1934.
- (18) Lightfoot, P. D.; Cox, R. A.; Crowley, J. N.; Destriau, M.; Hayman, G. D.; Jenkin, M. E.; Moortgat, G. K.; Zabel, F. *Atmos. Environ.* **1992**, *26A*, 1805.

Received for review January 5, 1999. Revised manuscript received September 8, 1999. Accepted March 20, 2000.

ES9900095